F. 健康危険情報

特記すべきことなし。

G. 研究発表

発表論文

準備中（本研究は平成２１年度に開始された研究であり、現在その成果をまとめた論文を執筆中である）

学会発表

特になし

H. 知的財産権の出願・登録情報

特記すべきことなし

研究成果の刊行に関する一覧表

著者氏名	論文タイトル名	発表誌名
Minae Niwa, Atsushi Kamiya, Rina Murai, Ken-ichiro Kubo, Aaron J Gruber, Kenji Tomita, Lingling Lu, Shuta Tomisato, Hanna Jaaro-Peled, Saurav Seshadri, Hideki Hiyama, Beverly Huang, Kazuhisa Kohda, Yukihiro Noda, Patricio O'Donnell, Kazunori Nakajima, Akira Sawa, and Toshitaka Nabeshima	Knockdown of DISC1 by in utero gene transfer disturbs postnatal dopaminergic maturation in the frontal cortex and leads to adult behavioral deficits.	***Neuron***, 65 (4), 480-489 (2010).

Cell PRESS

Neuron
Article

Knockdown of DISC1 by In Utero Gene Transfer Disturbs Postnatal Dopaminergic Maturation in the Frontal Cortex and Leads to Adult Behavioral Deficits

Minae Niwa,[1,2,3,11] Atsushi Kamiya,[1,11] Rina Murai,[2,4] Ken-ichiro Kubo,[5] Aaron J. Gruber,[6] Kenji Tomita,[5] Lingling Lu,[2] Shuta Tomisato,[7] Hanna Jaaro-Peled,[1] Saurav Seshadri,[1] Hideki Hiyama,[1] Beverly Huang,[1] Kazuhisa Kohda,[7] Yukihiro Noda,[8] Patricio O'Donnell,[6] Kazunori Nakajima,[5] Akira Sawa,[1,9,*] and Toshitaka Nabeshima[2,4,10,*]

[1]Department of Psychiatry and Behavioral Sciences, Johns Hopkins University School of Medicine, Baltimore, MD 21287, USA
[2]Department of Chemical Pharmacology, Meijo University, Nagoya 4688503, Japan
[3]Department of Psychiatry
[4]Department of Neuropsychopharmacology and Hospital Pharmacy
Nagoya University Graduate School of Medicine, Nagoya 4668560, Japan
[5]Department of Anatomy, Keio University School of Medicine, Tokyo 1608582, Japan
[6]Department of Anatomy and Neurobiology, University of Maryland School of Medicine, Baltimore, MD 21201, USA
[7]Department of Physiology, Keio University School of Medicine, Tokyo 1608582, Japan
[8]Division of Clinical Science and Neuropsychopharmacology, Meijo University, Nagoya 4688503, Japan
[9]Department of Neuroscience, Johns Hopkins University School of Medicine, Baltimore, MD 21287, USA
[10]The Academic Frontier Project for Private Universities, Comparative Cognitive Science Institutes, Nagoya 4688503, Japan
[11]These authors contributed equally to this work
*Correspondence: asawa1@jhmi.edu (A.S.), tnabeshi@ccmfs.meijo-u.ac.jp (T.N.)
DOI 10.1016/j.neuron.2010.01.019

SUMMARY

Adult brain function and behavior are influenced by neuronal network formation during development. Genetic susceptibility factors for adult psychiatric illnesses, such as Neuregulin-1 and Disrupted-in-Schizophrenia-1 (DISC1), influence adult high brain functions, including cognition and information processing. These factors have roles during neurodevelopment and are likely to cooperate, forming pathways or "signalosomes." Here we report the potential to generate an animal model via in utero gene transfer in order to address an important question of how nonlethal deficits in early development may affect postnatal brain maturation and high brain functions in adulthood, which are impaired in various psychiatric illnesses such as schizophrenia. We show that transient knockdown of DISC1 in the pre- and perinatal stages, specifically in a lineage of pyramidal neurons mainly in the prefrontal cortex, leads to selective abnormalities in postnatal mesocortical dopaminergic maturation and behavioral abnormalities associated with disturbed cortical neurocircuitry after puberty.

INTRODUCTION

Adult brain function and behavior are influenced by neuronal network formation during development. Consequently, disturbances of brain development are suggested to underlie the pathology of adult mental disorders, such as schizophrenia and mood disorders (Lewis and Levitt, 2002; Rapoport et al., 2005; Savitz and Drevets, 2009; Tenyi et al., 2009). Consistent with this notion, genetic susceptibility factors for these disorders that have been recently identified, including Neuregulin-1 and Disrupted-in-Schizophrenia-1 (DISC1), have roles during neurodevelopment and are likely to cooperate, forming molecular "pathways" (Harrison and Weinberger, 2005; Jaaro-Peled et al., 2009; Owen et al., 2005). Furthermore, many studies have indicated that variations of these disease susceptibility genes influence high brain functions, including cognition and information processing, in both normal subjects and patients (Kéri, 2009; Krug et al., 2008; Tomppo et al., 2009). Thus, these genetic factors are believed to be good probes to explore mechanistic links between brain development and adult brain functions.

Schizophrenia is a debilitating disorder with onset in young adulthood, although many lines of evidence have indicated that pre- and perinatal brain disturbances underlie the initial risks for the disease (Buka and Fan, 1999; McNeil, 1995). It is possible that these initial risks may in turn affect postnatal brain maturation, resulting in the delayed onset of the disorder. Prodromal stages of schizophrenia in adolescence and young adulthood may reflect the dynamic pathophysiology of disturbed brain maturation (Cannon et al., 2003; Jaaro-Peled et al., 2009; White et al., 2006). Some excellent longitudinal studies with clinical subjects have attempted to address this question (White et al., 2006). Nonetheless, good animal models that can depict the sequential changes from the initial disturbances in early brain development to defects of postnatal brain maturation, leading to adult brain dysfunction associated with schizophrenia, are awaited to permit dissection and understanding of the molecular mechanisms during the course of disease progression. Mice with manipulations of genetic susceptibility factors for the disease may provide this opportunity (Chen et al., 2006). Once available, such models may shed light on the pathological

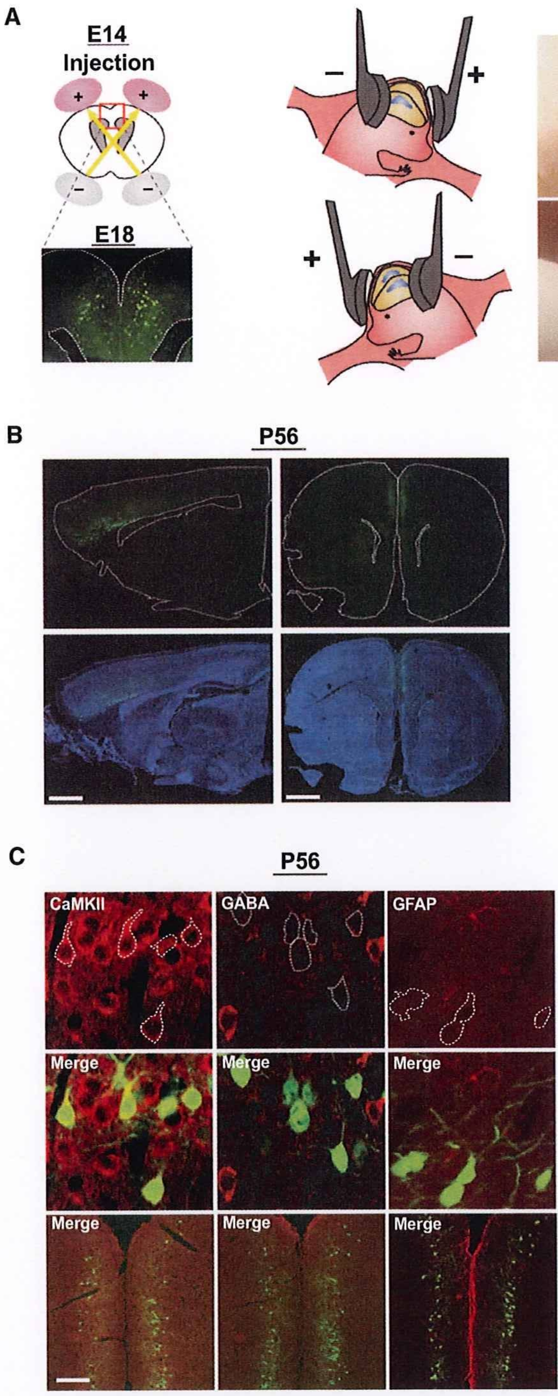

Figure 1. Selective Targeting of Constructs to Cells in a Lineage of Pyramidal Neurons in the Prefrontal Cortex via In Utero Gene Transfer

(A) Schematic representation of bilateral in utero injection of constructs followed by their incorporation by electroporation into progenitor cells in the ventricular zone at embryonic day 14 (E14). Migrating cells with GFP are visualized at E18 after injection of a GFP expression construct.

(B) Representative coronal and sagittal images of brains with GFP expression at P56 after injection of a GFP expression construct at E14. Blue, nucleus. The scale bars represent 1 mm.

(C) GFP-positive neurons in layers II/III at postnatal day 56 (P56) in mPFC. Most cells with GFP expression are CaMKII-positive pyramidal neurons (red in left panels), but not GABA (red in middle panels) or GFAP positive (red in right panels) at P56. The scale bar represents 100 μm.

mechanisms for schizophrenia. Furthermore, even more importantly, these models may clarify how minor or nonlethal brain disturbances in early development, possibly related to a combination of genetic variations, may affect high brain functions in adults, including cognition and information processing, in a wide range of mental conditions and even in subjects who may not be classified as having psychiatric disorders as defined by the Diagnostic and Statistical Manual of Mental Disorders.

Here we provide evidence to support the feasibility of in utero gene transfer to produce mouse models to address this question. In the present study, by utilizing this technique, we generated mice in which selective knockdown of DISC1 is achieved in a lineage for pyramidal neurons mainly in the prefrontal cortex (PFC), but only during development, which leads to maturation-dependent deficits in mesocortical dopaminergic projections and associated behavioral changes, including those in information processing and cognition.

RESULTS

Application of In Utero Gene Transfer to Modulate Expression of Target Genes in the Prefrontal Cortex

To evaluate the feasibility of the in utero gene transfer technique to analyze the modulation of gene expression in the PFC, an expression construct of green fluorescent protein (GFP) was injected into bilateral lateral ventricles and incorporated by electroporation into progenitor cells in the ventricular zone at embryonic day 14 (E14) in mice (Figure 1A; see Figure S1A available online). We analyzed sagittal and serial coronal sections from six randomly selected brains at postnatal day 56 (P56), and found that GFP-positive cells were located at +2.34 mm to ~+0.98 mm relative to Bregma, especially in the dorsolateral prefrontal cortex (DLPFC), medial prefrontal cortex (mPFC), orbitofrontal cortex (OFC), and anterior cingulate cortex (Figures 1B, S1B, and S1C). Thus, this method allows for gene targeting mainly into

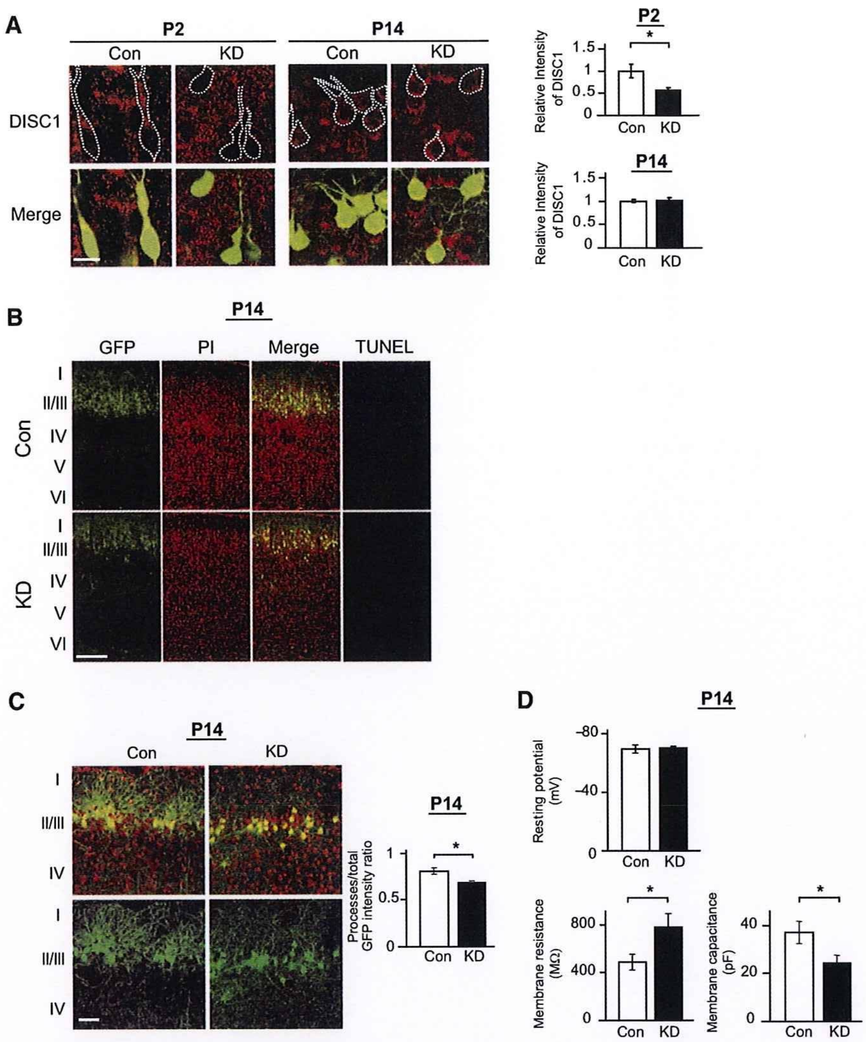

Figure 2. Mice with Knockdown of DISC1 in Pyramidal Neurons of the Prefrontal Cortex during Early Development via In Utero Gene Transfer Display Dendritic Abnormalities at P14

(A) Suppression of DISC1 immunoreactivity (red) in GFP-positive neurons is observed at P2, but not at P14, when shRNA to DISC1 is introduced (DISC1 knockdown [KD]) at E14 ($^*p < 0.05$). A total of 30 GFP-positive cells from cortical slices of three DISC1 KD mice and those of three control mice with scrambled/control shRNA was analyzed and compared. The scale bar represents 10 μm.

(B) GFP-positive neurons with RNAi at layers II/III at P14 after injection at E14. KD mice display dendritic pathology without signs of apoptosis (TUNEL), consistent with our previous publication (Kamiya et al., 2005). Red, nucleus. The scale bar represents 100 μm.

(C) Reduction of GFP fluorescence intensity in dendrites relative to total GFP fluorescence intensity in mPFC of KD mice at P14, compared to those of Con mice ($^*p < 0.05$, n = 5 per condition), suggesting impaired dendritic formation in KD mice. Red, nucleus. The scale bar represents 50 μm.

(D) Electrophysiological characteristics of pyramidal neurons with knockdown of DISC1 (majority of green cells) at layers II/III in mPFC at P14. Membrane resistance at −80 mV and membrane capacitance of GFP-positive neurons in DISC1 KD mice are significantly different compared with those in Con mice ($^*p < 0.05$), whereas there is no difference in resting potential in these two groups (n = 5 per condition).

Data are expressed as mean ± SEM.

the PFC. In the developing cerebral cortex, pyramidal neurons migrate radially from the ventricular zone, whereas interneurons migrate tangentially from ganglionic eminence into the developing cerebral wall (Anderson et al., 1997; Marin and Rubenstein, 2003). Glial lineages originating from the subventricular zone are produced at late embryonic and early postnatal days (E17 to P14) (Sauvageot and Stiles, 2002). Therefore, the constructs are likely to be integrated into cells in a lineage of pyramidal neurons. Indeed, GFP-positive cells were confined only to pyramidal neurons, around 20% of which were GFP positive in layers II/III at P56 (Figure 1C). These results indicate that in utero gene transfer can be used for modulating target gene expression mainly in pyramidal neurons in PFC during brain development.

Transient Knockdown of DISC1 in PFC during Development via In Utero RNAi Transfer

In this study, we used DISC1 as a probe to address how molecular disturbance in cells of the pyramidal neuron lineage in PFC during early development might influence postnatal brain maturation and adult phenotypes. Thus, we injected a well-characterized DISC1 short-hairpin RNA (shRNA) together with a GFP expression construct at E14 according to the protocol described above, and confirmed targeting to PFC. Histological phenotypes in the developing cortex elicited by this shRNA (defects in neuronal progenitor proliferation, delay in neuronal migration, and resultant changes in arborization) are consistent with those elicited by other shRNAs to DISC1 thus far reported (Kamiya et al., 2005; Mao et al., 2009), and are rescued by overexpression of wild-type DISC1 ($DISC1^R$) (Figure S2A). Suppression of DISC1 seems to be transient, confirmed by knockdown of DISC1 for at least 7 days after injection, but not after 3 weeks (Figure 2A). In the present study, we have characterized the DISC1 knockdown-elicited phenotypic changes at P14 in greater detail, by extending our previous observation (Kamiya et al., 2005). As the result of the transient *k*nock*d*own of DISC1 via RNA interference (RNAi) (designated DISC1 KD in this manuscript), GFP-positive pyramidal neurons were found in layers II/III without signs of apoptosis and with abnormal dendritic morphology (Figures 2B, 2C, and S2B–S2D). Impaired dendritic development in layers II/III at P14 in DISC1 KD mice was also functionally confirmed by electrophysiological approaches (Figure 2D).

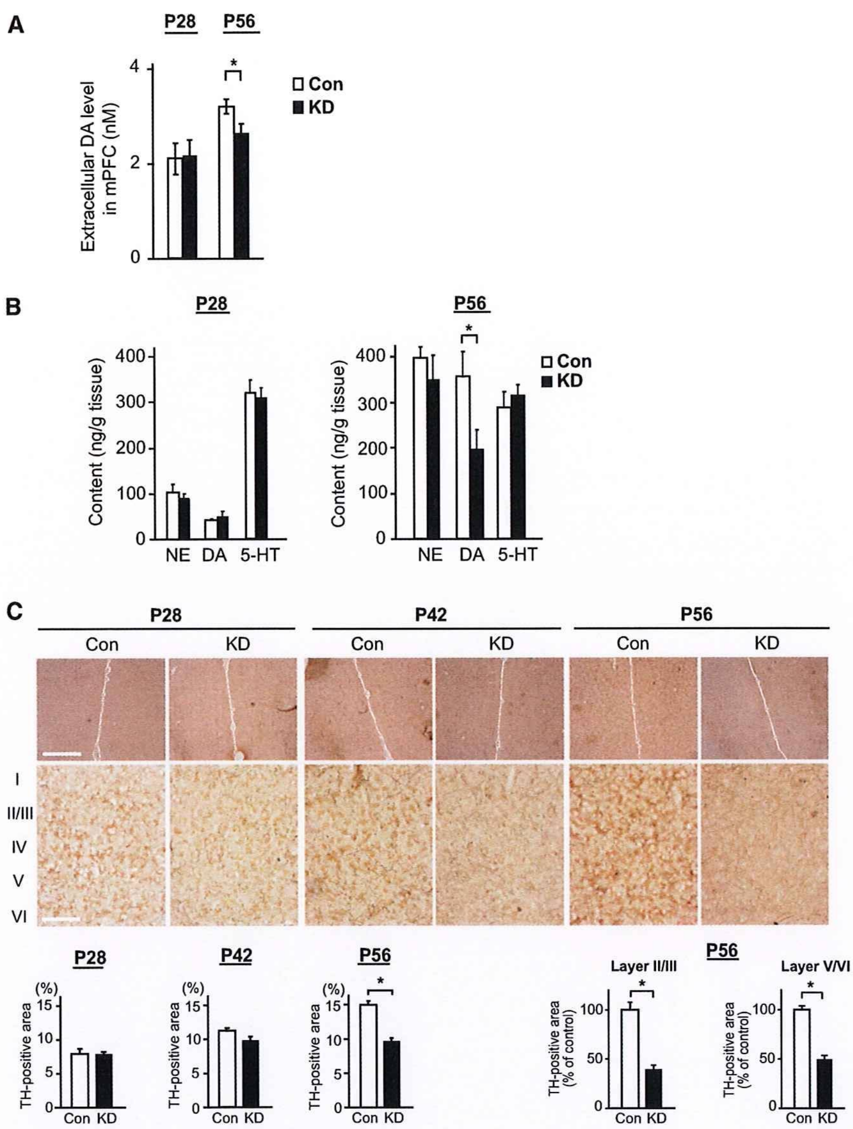

Figure 3. Disturbance in Postnatal Maturation of Mesocortical Dopaminergic Projections to the Medial Prefrontal Cortex in DISC1 Knockdown Mice

(A) Basal levels of extracellular dopamine (DA) in mPFC were analyzed by in vivo microdialysis, and a decrease in DISC1 KD mice compared with that in Con mice was detected at P56, but not at P28 (*$p < 0.05$, n = 6 per condition).

(B) Monoamine content in the frontal cortex as measured by HPLC. The level of DA in FC is decreased in DISC1 KD mice compared with that in Con mice at P56, but not at P28 (*$p < 0.05$, n = 7 per condition). No difference in the levels of NE and 5-HT is observed at these two time points.

(C) Immunostaining of tyrosine hydroxylase (TH) in mPFC, including prelimbic and infralimbic cortex (upper panels, low magnification; bottom panels, high magnification). TH level in mPFC is relatively decreased in KD mice compared with Con mice at P56 (*$p < 0.05$, n = 6 per condition) in both layers II/III and V/VI, whereas there is no difference between KD and Con at P28 and P42. The scale bar in low-magnification pictures represents 200 μm, and in high-magnification pictures represents 500 μm.

Data are expressed as mean ± SEM.

Disturbance in Postnatal Maturation of Mesocortical Dopaminergic Projections and Interneurons to the Medial Prefrontal Cortex in DISC1 KD Mice

Next, we addressed whether the dendritic abnormalities at P14 elicited by transient knockdown of DISC1 in the pre-/perinatal stages may later influence postnatal brain maturation. We first examined differences in body weight between DISC1 KD and control mice at P14, P28, and P56, which may reflect atypical developmental trajectories and could potentially affect maturation of neuronal circuits and behavior nonspecifically, but no difference in body weight was observed between these two groups (Figure S3A). At the histological level, we did not find any robust differences in Nissl staining in mPFC at P28 and P56 (Figure S3B). No difference between DISC1 KD and controls in immunostaining and western blotting for glial fibrillary acidic protein (GFAP) indicated that there was no gliosis in DISC1 KD mice at P28 and P56 (Figures S3C and S3D).

In contrast, we observed a marked decrease in the extracellular levels of dopamine in mPFC, measured by microdialysis, and total content of dopamine between KD and controls in FC at P56 but not at P28 (Figures 3A and 3B), whereas no changes were observed in total content of dopamine in other brain areas including nucleus accumbens, hippocampus, and cerebellum (Figure S3E). This change may be specific to dopamine, as no changes in glutamate, norepinephrine (NE), or serotonin were observed (Figure 3B, S3E, and S3F). Increase in the level of dopamine from birth to adolescence in the frontal cortex is known to reflect physiological maturation of the dopaminergic projection (Benes et al., 2000; Goto and Grace, 2007; Rosenberg and Lewis, 1995). Insufficient elevation of dopamine at P56 in DISC1 KD mice may indicate disturbed maturation of dopaminergic neurons. Consistent with this idea, relative immunoreactivity against tyrosine hydroxylase (TH), a marker of mature axon terminals of the dopaminergic projection, was decreased in both layers II/III and V/VI at P56, but not at P28 and P42, in DISC1 KD compared to control mice (Figure 3C). This relative decrease of TH was also confirmed by western blotting (Figure S3G). In contrast, we did not observe changes in expression of dopamine receptor-1 (D1R) and -2 (D2R) (Figures S3G and S3H).

Given that there are inter- and intralaminar connections of pyramidal neurons and GABAergic interneurons in local circuits in PFC where mesocortical dopaminergic neurons also have synaptic contact (Sesack et al., 2003), this aberrant development

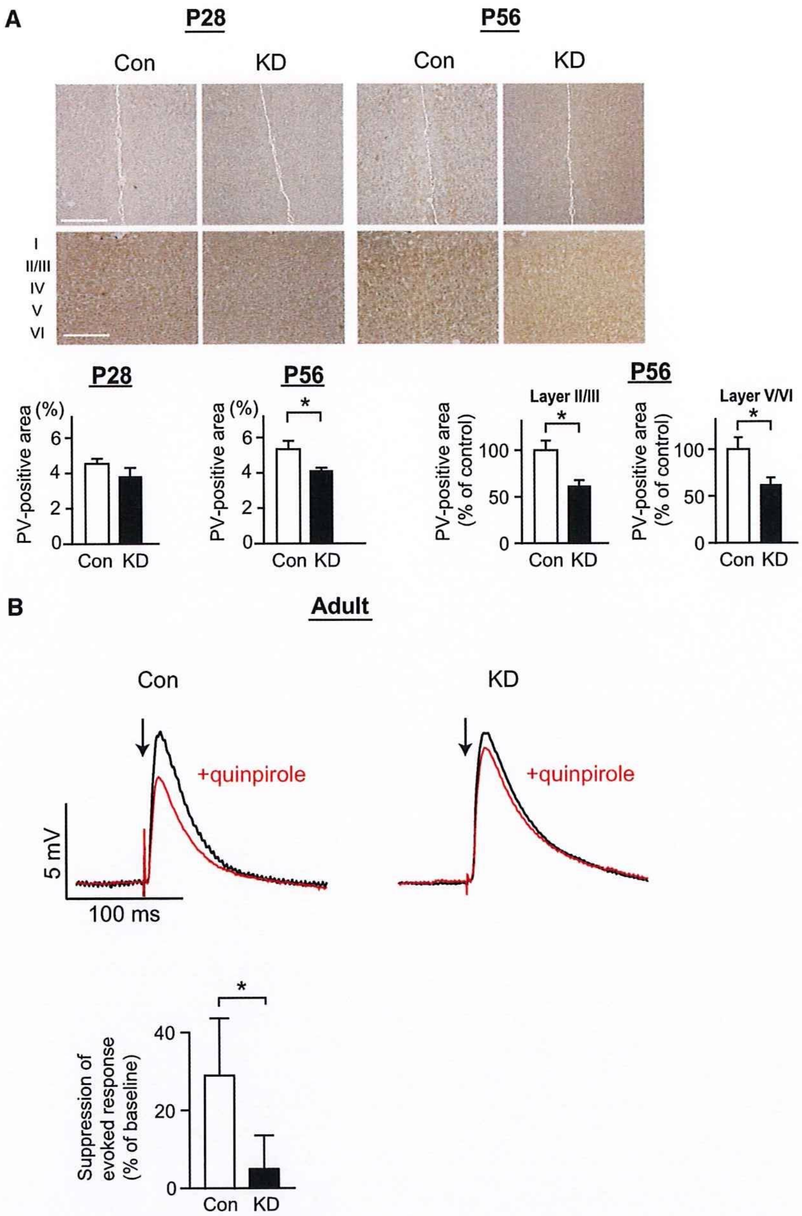

Figure 4. Disturbances of Interneurons and Pyramidal Neurons in PFC of DISC1 KD Mice after Puberty

(A) Immunostaining of parvalbumin (PV) in the mPFC (upper panels, low magnification; bottom panels, high magnification). Immunoreactivity of PV is quantified under each condition (lower graphs). The expression levels of PV in the mPFC (both layers II/III and V/VI) are decreased in KD mice compared with Con mice at P56, but not at P28 (*$p < 0.05$, n = 6 per condition). The scale bar in low-magnification pictures represents 200 μm, and in high-magnification pictures represents 500 μm.

(B) Electrophysiological responses of PFC pyramidal neurons to electrical stimulation recorded using the whole-cell patch-clamp technique in acute slices from young adult male mice. Overlay of membrane potential responses evoked with electrical stimulation of cortico-cortical fibers before (black trace) and during (red trace) bath application of the D2 dopamine agonist quinpirole (5 μM) in KD and Con mice. Arrows indicate times of single-pulse stimulation. Quinpirole attenuation of evoked excitatory postsynaptic potentials is reduced in KD mice (*$p < 0.05$, n = 5 per condition).

Data are expressed as mean ± SEM.

of the pyramidal neurons may affect GABAergic interneurons. To test this possibility, we examined the expression level of parvalbumin, a marker of the fast-spiking GABAergic interneurons. We observed reduction of parvalbumin immunoreactivity in layers II/III and V/VI in mPFC in DISC1 KD mice at P56 but not at P28, suggesting that there is a possible deficit of interneurons in adulthood; this effect is likely to occur during postnatal brain maturation (Figure 4A). To test whether dopamine regulation of local circuit processing in mPFC is altered in adult DISC1 KD mice, we recorded deep-layer pyramidal neurons by using the whole-cell patch-clamp technique in acute brain slices (Figure S4). Neither resting membrane potential nor input resistance was different from controls, indicating that basic somatic electrophysiological properties are not grossly disrupted in adult DISC1 KD mice (data not shown). Nonetheless, bath application of the D2R dopamine receptor agonist quinpirole attenuated electrically evoked membrane responses in control mice, but such attenuation was markedly reduced in DISC1 KD mice (Figure 4B). Taken together, these results suggest that neonatal pyramidal neuron deficits elicited by pre-/perinatal knockdown of DISC1 lead to overall disturbances in circuitry involving dopamine neurons, pyramidal neurons, and interneurons, manifested only after puberty.

Behavioral Deficits in DISC1 KD Mice after Puberty

We then questioned whether such neurochemical and physiological disturbance in postnatal brain maturation might result in behavioral deficits. Prepulse inhibition (PPI) reflects sensory gating function, a major indicator of information processing involving the cortex, which is also frequently impaired in various mental illnesses (Arguello and Gogos, 2006). DISC1 KD mice at P56, but not at P28, displayed decreased PPI, in comparison with controls (Figure 5A). DISC1-associated PPI deficits are further confirmed in mice by another shRNA to DISC1 that knocks down this molecule to a lesser extent than does the shRNA mainly used in this study (Kamiya et al., 2005, 2008; Mao et al., 2009): milder deficits in PPI that were consistent with the milder effect on DISC1 expression were observed in the mice (Figure S5A). We also tested the effect of clozapine, which is reported to elevate dopamine levels via blocking the D2 autoreceptor (Rayevsky et al., 1995). Very interestingly, when we administered clozapine acutely to DISC1 KD mice, we observed

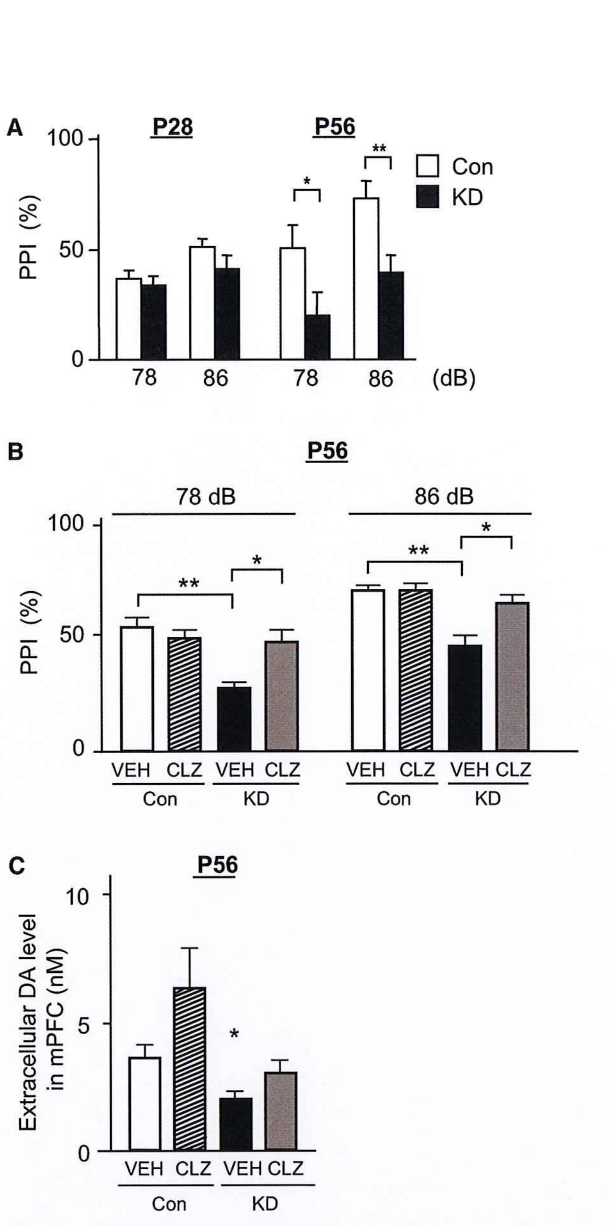

Figure 5. Attenuation of Prepulse Inhibition Deficits by Treatment with Clozapine in DISC1 KD Mice after Puberty

(A) Performance in prepulse inhibition (PPI) at P28 and P56. Impairment of PPI is observed in DISC1 KD mice at P56, but not at P28 (*$p < 0.05$, **$p < 0.01$, $n = 12$ per condition).

(B) Effect of clozapine (CLZ) on the impairment of PPI in KD mice at P56. Treatment with CLZ (3 mg/kg, i.p.) ameliorates the impairment of PPI in KD mice at P56 (*$p < 0.05$, **$p < 0.01$, $n = 16$ per condition). VEH, vehicle.

(C) Effect of CLZ on extracellular DA levels in mPFC by in vivo microdialysis. Administration of CLZ (3 mg/kg, i.p.) elevates extracellular DA levels in mPFC in both Con and KD mice at P56 (*$p < 0.05$, $n = 4$ per condition).

Data are expressed as mean ± SEM.

normalized levels of dopamine in mPFC and improvement of PPI deficits, without alterations in the startle amplitude (Figures 5B, 5C, S5B, and S5C). These results suggest that PPI deficits in DISC1 KD mice are, at least in part, associated with decreased levels of dopamine in the mPFC at P56.

The novel object recognition task (NORT) measures functions of the hippocampus and the cortex, including functions associated with visual working memory (Ozawa et al., 2006). No difference was observed in exploratory preference during the training between control and KD mice, suggesting that there were no significant differences in curiosity and/or motivation to explore objects between the two groups (Figure S5D). In contrast, KD mice at P56, but not at P28, displayed impaired performance in the test runs 24 hr after the training session, whereas no difference was found 1 hr after the training session (Figures S5D and S5E). Acute administration of clozapine improved their performance in NORT (Figure S5F). To address a function more specific to the cortex, mice were assessed by a T maze test at P56. DISC1 KD mice showed significantly fewer correct choices than did control mice, with delay intervals of 15 s, although there was no difference in required training time between the two groups (Figure S5G). In contrast, no difference was observed between DISC1 KD and control mice in the forced-swim test, a paradigm associated with depression (Figure S5H).

Next, in order to examine dopamine-associated behavioral deficits in DISC1 KD mice further, we challenged DISC1 KD mice with the psychostimulant methamphetamine. Although DISC1 KD mice did not differ from controls in spontaneous locomotion in the open field (Figure S6), DISC1 KD mice at P56, but not at P28, displayed hypersensitivity to administration of methamphetamine in locomotion (Figure 6A). Consistent with this result, we found that the increase of extracellular dopamine levels in nucleus accumbens in DISC1 KD mice was higher than that in controls after the administration of methamphetamine, although the basal levels of extracellular dopamine were slightly lower in DISC1 KD mice than in controls (Figure 6B).

DISCUSSION

There are two major conclusions in the present study. First, we report the potential to generate an animal model via in utero gene transfer in order to address an important question of how nonlethal deficits in early development may affect postnatal brain maturation of information processing and cognition in adulthood. Second, we show that transient knockdown of DISC1 in the pre- and perinatal stages, specifically in a lineage of pyramidal neurons mainly in PFC, leads to abnormalities in postnatal mesocortical dopaminergic maturation which results in overall disturbance in circuitry and several behavioral abnormalities in adulthood. Although there is precedence that insults in early development lead to delayed phenotypic manifestations in rodents (Koshibu et al., 2005; Lipska et al., 1993; Moore et al., 2006), the present study indicates the sequential link among pre-/perinatal disturbance in a specific genetic susceptibility factor (DISC1), the associated dendritic abnormalities in the neonatal stage, and, in turn, selective phenotypes in adolescence and adulthood.

This study may aid molecular understanding of how initial insults during early development disturb postnatal brain maturation for many years which results in full-blown onset of schizophrenia after puberty (Buka and Fan, 1999; Jaaro-Peled et al., 2009; McNeil, 1995). Although it is still being debated, brains from patients with schizophrenia show abnormalities in the cortex, especially in layers II/III, which include decreased arborization and smaller size of pyramidal neurons, as well as alteration

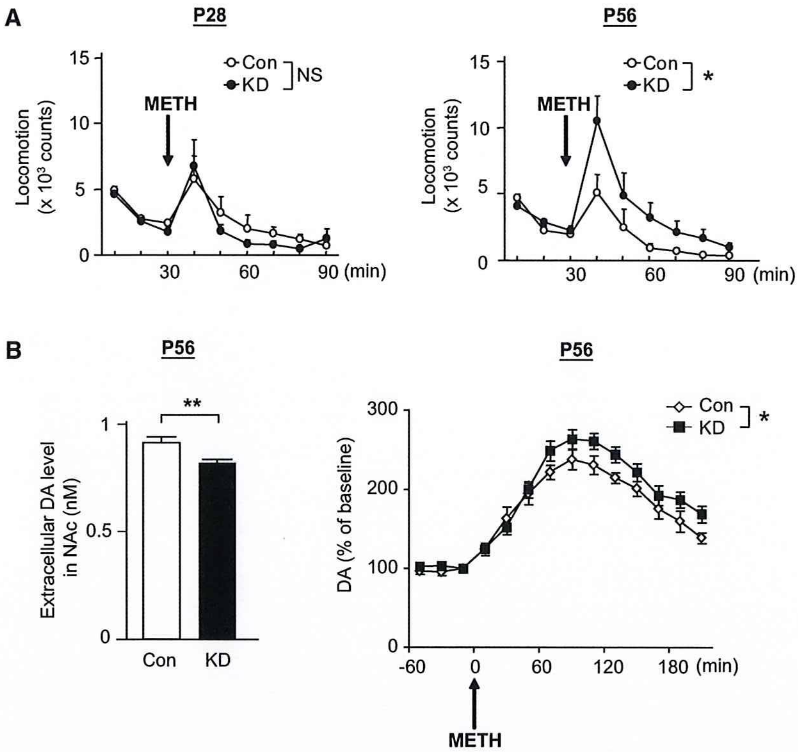

Figure 6. Hypersensitivity to the Psychostimulant Methamphetamine in DISC1 KD Mice after Puberty

(A) Methamphetamine (METH; 1 mg/kg, s.c.) -induced hyperactivity is augmented in DISC1 KD mice compared with Con mice, at P56 but not at P28 (*$p < 0.05$, $n = 6$–10 per condition).

(B) The extent of increase after METH challenge in levels of extracellular DA relative to those at the baseline is augmented in the nucleus accumbens (NAc) of DISC1 KD mice compared with Con mice at P56 (*$p < 0.05$, $n = 8$ per condition) (right), whereas mild but significant reduction of basal levels of extracellular DA is observed in KD mice (**$p < 0.01$, $n = 8$ per condition) (left).

Data are expressed as mean ± SEM.

in a subset of interneurons (Akbarian et al., 1995; Benes and Berretta, 2001; Glantz and Lewis, 2000; Guidotti et al., 2000; Lewis et al., 2005; Selemon and Goldman-Rakic, 1999). Furthermore, a decrease in tyrosine hydroxylase staining in schizophrenia patients has been reported, suggesting a reduction of dopaminergic innervation in the prefrontal cortex in schizophrenia (Akil et al., 1999). Primary defects for these cytoarchitectural changes may occur during neurodevelopment, because they are not accompanied by gliosis. Nevertheless, it has been unclear what kinds of neurodevelopmental defects result in such brain anatomical changes in patients with schizophrenia, with clinical onset 15–30 years after birth, characterized by psychosis and impaired cognition and information processing, and associated with aberrant neurotransmission, especially dopaminergic neurotransmission. The model in this study represents a majority of these objective characteristics reported in schizophrenia research. Therefore, to address the hierarchy and mechanistic links of these characteristics, this DISC1 model produced via in utero gene transfer may be useful. For example, an important question for future mechanistic studies with this model is how a decrease in tyrosine hydroxylase in all layers, or disturbance of postnatal maturation of mesocortical dopaminergic projections, is induced by dendritic abnormalities of the pyramidal neurons in layer II/III in the cortex in early development. Another question is how dysfunction of mesocortical dopaminergic projection affects its mesolimbic circuitry, including possible changes in dynamics of dopamine uptake and release, in the nucleus accumbens.

Although various types of genetically engineered animals, including inducible and conditional systems, have been developed, the in utero gene transfer technique with expression and/or shRNA constructs for RNAi may be a promising alternative methodology. We can select the target cell populations for genetic modulation specifically, by changing the direction of the electroporation (LoTurco et al., 2009). Thus, preferential targeting to a lineage of interneurons in the cortex or to hippocampal neurons is also technically feasible by targeting the electrodes toward ganglionic eminence or medial regions of the embryonic telencephalon, respectively (Borrell et al., 2005; Navarro-Quiroga et al., 2007). Furthermore, introduction of inducible expression constructs in in utero gene transfer will allow us to have better control of target gene expression (LoTurco et al., 2009; Manent et al., 2009; Matsuda and Cepko, 2007).

Many investigators have considered the possibility that adult brain function and behavior are influenced by neuronal network formation during development (Cannon et al., 2003; Harrison and Weinberger, 2005; Jaaro-Peled et al., 2009; Lisman et al., 2008), which is modulated by a combination of several genetic and environmental factors, and the concept of "pathway(s)" is more likely to mimic the mechanisms than the effect of a single gene product. By using the technical advantage of in utero transfer in which expression of more than one gene can be modified at one time by cotransfection of expression and/or RNAi constructs (Kamiya et al., 2008; Shu et al., 2004; Tsai et al., 2005; Young-Pearse et al., 2007), we will be able to test the synergistic influence or epistatic effect of multiple genetic factors. In a more general application, we propose that this method is useful in testing how modest but significant defects in neuronal network formation in early development lead to adult behavioral traits; furthermore, if potential variation between batches and animals is well controlled, this technique may also be utilized in trying to build novel animal models for various adult mental disorders, including schizophrenia, in which multiple risk factors play etiological roles during neurodevelopment.

EXPERIMENTAL PROCEDURES

Constructs

Short-hairpin RNA (shRNA) to DISC1 (5′-GGCAAACACTGTGAAGTGC-3′) was expressed by an H1 promoter-driven pSuper plasmid (Brummelkamp et al., 2002). This shRNA was shown to effectively knock down DISC1 in cell cultures and in vivo via in utero gene transfer in previous publications from more than one research group (Kamiya et al., 2005, 2008; Mao et al., 2009). The duration of knockdown expression of genes by this H1-driven pSuper plasmid is dependent on the target molecules that we have tested so far (data not shown), and suppression of DISC1 was clearly transient in the developing cortex. Scrambled target sequence without homology to any known messenger RNA was used to produce the control RNAi. The expression construct used for rescue control experiments ($DISC1^R$) is described in Supplemental Information. The GFP expression construct is under the control of the CAG promoter.

In Utero Electroporation

In utero electroporation was performed by our published protocol with some modifications (Kamiya et al., 2005; Tabata and Nakajima, 2001). We used ICR mice, because neuropathological changes induced by the same shRNA to DISC1 had been characterized in this strain (Kamiya et al., 2005, 2008). Pregnant mice were anesthetized at E14 by intraperitoneal administration of 2,2,2-tribromoethanol in tert-amyl alcohol (0.4 mg/g). Two centimeter midline laparotomy was performed and the uterine horn was exposed. RNAi plasmids (2 μg/μl) together with GFP expression vector with CAG promoter (1 μg/μl) (molar ratio approximately 3:1) were injected into the bilateral ventricles with a glass micropipette made from a microcapillary tube (GD-1; Narishige). Injected plasmid solution contained Fast Green solution (0.001%) to monitor the injection. The embryo's head in the uterus was held between the tweezers-type electrode consisting of two disc electrodes of 5 mm diameter (CUY650-5; Tokiwa Science). Depending on which hemisphere was injected, the electrodes were oriented at a rough 20° outward angle from the midline and a rough 30° angle downward from an imaginary line from the olfactory bulbs to the caudal side of the cortical hemisphere. Electrode pulses (35V; 50 ms) were charged five times at intervals of 950 ms with an electroporator (CUY21E; Tokiwa Science). The uterine horn was placed back into the abdominal cavity and the abdominal wall and skin were sutured. All experiments were performed in accordance with the institutional guidelines for animal experiments.

Histology and Quantitative Analyses

Histological procedures were performed as previously described (Kamiya et al., 2005) with minor modifications. Brains were fixed with 4% paraformaldehyde, and coronal sections, including mPFC, were obtained with a cryostat at 20 μm (CM 1850; Leica). For immunohistochemistry, the following primary antibodies were used: anti-DISC1 (1: 100) (Ozeki et al., 2003), anti-tyrosine hydroxylase (TH) (1:100; Millipore), anti-parvalbumin (PV) (1:100; Sigma-Aldrich), anti-CaMKII (1:200; Upstate Biotechnology), and anti-GABA (1:200; Sigma-Aldrich). Fluorescent secondary antibodies conjugated to Alexa 488 and Alexa 568 (Molecular Probes) as well as biotin-conjugated secondaries were used for chromogen detection. Nuclei were labeled with Neurotrace Nissl 530/615 (Molecular Probes), propidium iodide (Molecular Probes), or DAPI (Molecular Probes). TUNEL staining was carried out as published (Yu et al., 2003).

To evaluate which types of cells were targeted by in utero gene transfer, the number of double-labeled cells with GFP together with specific cell markers, such as CaMKII (for pyramidal neurons), GABA (for interneurons), and GFAP (for astrocytes), was counted in a region of interest defined as 100 μm wide × 50 μm high in layers II/III in mPFC. Two regions of interest were randomly selected from three mice (a total of six regions). Images were acquired with a confocal microscope (LSM510; Carl Zeiss). The ratio of the number of double-labeled cells to that of cells with each cell marker was measured.

In order to quantify the effect of RNAi on expression of DISC1, the immunofluorescent intensity of DISC1 signal in each GFP-positive cell was measured by using MetaMorph software version 7.1 (MDS Analytical Technologies) after images were acquired with a confocal microscope (LSM510). The acquisition parameters were kept the same for all images. The intensity of the signal from randomly selected 10 GFP-positive cells in layers II/III of mPFC was quantitatively assessed in three DISC1 KD and three Con mice (i.e., 30 cells from DISC1 KD and 30 cells from Con mice). The signal in a region of equal size without cells in the lateral ventricle was subtracted as background.

To quantify immunoreactivity of TH and PV, a region of interest was defined as 800 μm wide × 1300 μm high in mPFC in the coronal sections (anteroposterior [AP]: +1.98 to +1.54 mm; mediolateral (ML): ± 0.8 mm from Bregma; dorsoventral [DV]: −1.75 to −3.05 mm from the dura) according to the atlas of Franklin and Paxinos (2007). Three images were acquired with a light microscope (Axioskop2 plus; Carl Zeiss) for each brain (six brains per DISC1 KD and control mice). The acquisition parameters were kept the same for all images. The areas of TH- or PV-positive cells/mm^2 were measured by the imaging software Win-Roof (Mitani) after subtraction of the threshold value. The threshold was automatically measured at a minimum level by this software in the first image from a control mouse sample at P28 and was kept constant across all images.

For the procedures of morphological analysis of dendrites, see Supplemental Experimental Procedures.

Microdialysis

Microdialysis was carried out as previously described (Niwa et al., 2007) with a minor modification. A guide cannula (AG-6; Eicom) was implanted into the mPFC (15° angle from AP: +1.7 mm; ML: −1.0 mm from Bregma; DV: −1.5 mm from the dura) or nucleus accumbens (AP: +1.7 mm; ML: −0.8 mm from Bregma; DV: −4.0 mm from the dura). Ringer's solution (147 mM NaCl, 4 mM KCl, and 2.3 mM $CaCl_2$) was continuously perfused (1.0 μl/min). The dialysates were collected every 10 min and analyzed by high-performance liquid chromatography (HPLC) (Eicom). The levels of dopamine were also analyzed after the intraperitoneal injection of clozapine (3 mg/kg) (Sigma-Aldrich) or subcutaneous injection of methamphetamine (METH) (1 mg/kg) (Dainippon Sumitomo).

High-Performance Liquid Chromatography

Brains were removed rapidly, and each brain region was dissected out on ice according to the atlas of Franklin and Paxinos (2007). The brain homogenates were centrifuged at 20,000 × *g* for 15 min at 4°C, and the supernatants were mixed with 1 M sodium acetate to adjust to pH 3.0 for analysis by HPLC and by electrochemical detector (Eicom). The contents of norepinephrine (NE), dopamine (DA), and 5-hydroxytryptamine (5-HT) were determined as previously described (Miyamoto et al., 2002).

Electrophysiology

Mice were perfused with ice-cold artificial cerebrospinal fluid (ACSF) containing 125 mM NaCl, 25 mM $NaHCO_3$, 10 mM glucose, 3.5 mM KCl, 1.25 mM NaH_2PO_4, 0.5 mM (for P14) or 0.1 mM (for adult stage) $CaCl_2$, and 3 mM $MgCl_2$ (pH 7.4); osmolarity 285–295 mOsm. Coronal slices of brains at 400 μm (AP: +1.7 to 2.1 mm from Bregma) were made on a Vibratome and incubated in ACSF solution (35°C) oxygenated with 95% O_2 and 5% CO_2 for 60–70 min. For the recording ACSF, $CaCl_2$ was increased to 2 mM and $MgCl_2$ was decreased to 1 mM. All experiments were conducted at 33°C–35°C.

At P14, whole-cell recordings were performed from the GFP-labeled pyramidal neurons in layers II/III in the mPFC. Patch pipettes (3–6 MΩ) were filled with 115 mM K gluconate, 20 mM KCl, 10 mM KOH, 2 mM $MgCl_2$, 4 mM Na_2ATP, 1 mM NaGTP, 10 mM HEPES, 0.4 mM EGTA (pH 7.2). The τ_m was obtained by single-exponential fitting and the membrane capacitance was calculated.

At adult stage, whole-cell recordings were performed from pyramidal neurons in layers V/VI in the mPFC, where GFP-labeled cells were located in layers II/III, and identified under visual guidance by using infrared differential interference contrast video microscopy. Electrical stimulation (1 pulse, 0.2–1.4 mA) was applied through an electrode consisting of tungsten wire. The stimulating electrode was placed near layer I, 0.7–1 mm lateral to the location of whole-cell recordings in layers V/VI . Patch pipettes (9–12 MΩ) were filled with 115 mM K gluconate, 10 mM HEPES, 2 mM $MgCl_2$, 20 mM KCl, 2 mM MgATP, 2 mM Na_2ATP, and 0.3 mM GTP (pH 7.3); 285–295 mOsm. All bath-applied drugs, such as quinpirole and CNQX, were applied in the recording solution at known concentrations. Single pulses of current were delivered every 20 s, and stimulation current was adjusted so as to produce 4–10 mV postsynaptic potentials with reliable amplitude. Baseline responses to stimulation were recorded prior to adding quinpirole (5 μM) for 5–6 min. The magnitude of evoked responses was averaged over the baseline and compared to the average during the 5 min time interval from +2 to +7 min after quinpirole addition. This period was chosen for consistency, with differences revealed by previous investigations of D2 modulation of PFC activity in rodent models of schizophrenia (Tseng et al., 2008).

Behavioral Analysis

Prepulse Inhibition

Prepulse inhibition (Arguello and Gogos, 2006) of the acoustic startle response was measured using an SR-LAB System (San Diego Instruments). The stimulus onset consisted of a 20 ms prepulse, a 100 ms delay, and then a 40 ms startle pulse. The intensity of the prepulse was 8 or 16 dB above the 70 dB background noise. The amount of prepulse inhibition was calculated as a percentage of the 120 dB acoustic startle response: 100 – [(startle reactivity on prepulse + startle pulse)/startle reactivity on startle pulse] × 100. PPI tests were also performed 30 min after the intraperitoneal injection of clozapine (3 mg/kg).

Locomotor Activity

To measure spontaneous activity, mice were placed in a transparent acrylic cage, and locomotion and rearing were measured every 5 min for 60 min by using digital counters with infrared sensors (Scanet SV-10; Merquest) as described previously (Miyamoto et al., 2002). To measure methamphetamine (METH) -induced hyperactivity, mice received one subcutaneous injection of METH (1 mg/kg) after 30 min of prehabituation in a cage (Miyamoto et al., 2004).

Unbiased Assessment in Experimental Procedures

To avoid experimental bias by investigators, in utero surgery and all analyses, including those for DISC1 immunostaining and behavioral tests, were conducted by multiple investigators in a systematic manner as follows: an investigator conducted in utero surgery without knowing the identification of constructs. Furthermore, investigators conducted several assays without knowing the identification of mice (either DISC1 KD or controls).

Statistical Analysis

The Student's *t* test was used in comparing two sets of data. Statistical differences among more than three groups were determined using one-way analysis of variance (ANOVA), two-way ANOVA, or ANOVA with repeated measures followed by Bonferroni multiple comparison tests. A value of $p < 0.05$ was considered statistically significant. All data are expressed as mean ± SEM.

SUPPLEMENTAL INFORMATION

Supplemental Information includes six figures and Supplemental Experimental Procedures and can be found with this article online at doi:10.1016/j.neuron.2010.01.019.

ACKNOWLEDGMENTS

We thank Dr. Pamela Talalay and Dr. Eva Anton for critical reading and Ms. Yukiko Lema for organizing the manuscript. This work was supported by U.S. Public Heath Service grant MH-069853 (A.S.), Silvio O. Conte Center grants MH-084018 (A.S.) and MH-088753 (A.S.), and foundation grants from Stanley (A.S.), S-R (A.S., A.K.), RUSK (A.S.), and NARSAD (A.S., A.K., H.J.-P.). This work was also supported by grants from JSPS (T.N., K.N., M.N.), MEXT (T.N., K.N.), MARC (T.N.), MHLW (T.N., K.K.), Sumitomo (K.N.), Naito (K.N.), Academic Frontier Project (T.N.), and Takeda (T.N., K.N.).

Accepted: January 14, 2010
Published: February 24, 2010

REFERENCES

Akbarian, S., Kim, J.J., Potkin, S.G., Hagman, J.O., Tafazzoli, A., Bunney, W.E., Jr., and Jones, E.G. (1995). Gene expression for glutamic acid decarboxylase is reduced without loss of neurons in prefrontal cortex of schizophrenics. Arch. Gen. Psychiatry *52*, 258–266.

Akil, M., Pierri, J.N., Whitehead, R.E., Edgar, C.L., Mohila, C., Sampson, A.R., and Lewis, D.A. (1999). Lamina-specific alterations in the dopamine innervation of the prefrontal cortex in schizophrenic subjects. Am. J. Psychiatry *156*, 1580–1589.

Anderson, S.A., Eisenstat, D.D., Shi, L., and Rubenstein, J.L. (1997). Interneuron migration from basal forebrain to neocortex: dependence on Dlx genes. Science *278*, 474–476.

Arguello, P.A., and Gogos, J.A. (2006). Modeling madness in mice: one piece at a time. Neuron *52*, 179–196.

Benes, F.M., and Berretta, S. (2001). GABAergic interneurons: implications for understanding schizophrenia and bipolar disorder. Neuropsychopharmacology *25*, 1–27.

Benes, F.M., Taylor, J.B., and Cunningham, M.C. (2000). Convergence and plasticity of monoaminergic systems in the medial prefrontal cortex during the postnatal period: implications for the development of psychopathology. Cereb. Cortex *10*, 1014–1027.

Borrell, V., Yoshimura, Y., and Callaway, E.M. (2005). Targeted gene delivery to telencephalic inhibitory neurons by directional in utero electroporation. J. Neurosci. Methods *143*, 151–158.

Brummelkamp, T.R., Bernards, R., and Agami, R. (2002). A system for stable expression of short interfering RNAs in mammalian cells. Science *296*, 550–553.

Buka, S.L., and Fan, A.P. (1999). Association of prenatal and perinatal complications with subsequent bipolar disorder and schizophrenia. Schizophr. Res. *39*, 113–119.

Cannon, T.D., van Erp, T.G., Bearden, C.E., Loewy, R., Thompson, P., Toga, A.W., Huttunen, M.O., Keshavan, M.S., Seidman, L.J., and Tsuang, M.T. (2003). Early and late neurodevelopmental influences in the prodrome to schizophrenia: contributions of genes, environment, and their interactions. Schizophr. Bull. *29*, 653–669.

Chen, J., Lipska, B.K., and Weinberger, D.R. (2006). Genetic mouse models of schizophrenia: from hypothesis-based to susceptibility gene-based models. Biol. Psychiatry *59*, 1180–1188.

Franklin, B.J.K., and Paxinos, G. (2007). The Mouse Brain in Stereotaxic Coordinates (San Diego: Academic Press).

Glantz, L.A., and Lewis, D.A. (2000). Decreased dendritic spine density on prefrontal cortical pyramidal neurons in schizophrenia. Arch. Gen. Psychiatry *57*, 65–73.

Goto, Y., and Grace, A.A. (2007). The dopamine system and the pathophysiology of schizophrenia: a basic science perspective. Int. Rev. Neurobiol. *78C*, 41–68.

Guidotti, A., Auta, J., Davis, J.M., Di-Giorgi-Gerevini, V., Dwivedi, Y., Grayson, D.R., Impagnatiello, F., Pandey, G., Pesold, C., Sharma, R., et al. (2000). Decrease in reelin and glutamic acid decarboxylase67 (GAD67) expression in schizophrenia and bipolar disorder: a postmortem brain study. Arch. Gen. Psychiatry *57*, 1061–1069.

Harrison, P.J., and Weinberger, D.R. (2005). Schizophrenia genes, gene expression, and neuropathology: on the matter of their convergence. Mol. Psychiatry *10*, 40–68.

Jaaro-Peled, H., Hayashi-Takagi, A., Seshadri, S., Kamiya, A., Brandon, N.J., and Sawa, A. (2009). Neurodevelopmental mechanisms of schizophrenia: understanding disturbed postnatal brain maturation through neuregulin-1-ErbB4 and DISC1. Trends Neurosci. *32*, 485–495.

Kamiya, A., Kubo, K., Tomoda, T., Takaki, M., Youn, R., Ozeki, Y., Sawamura, N., Park, U., Kudo, C., Okawa, M., et al. (2005). A schizophrenia-associated mutation of DISC1 perturbs cerebral cortex development. Nat. Cell Biol. *7*, 1167–1178.

Kamiya, A., Tan, P.L., Kubo, K., Engelhard, C., Ishizuka, K., Kubo, A., Tsukita, S., Pulver, A.E., Nakajima, K., Cascella, N.G., et al. (2008). Recruitment of PCM1 to the centrosome by the cooperative action of DISC1 and BBS4: a candidate for psychiatric illnesses. Arch. Gen. Psychiatry *65*, 996–1006.

Kéri, S. (2009). Genes for psychosis and creativity: a promoter polymorphism of the neuregulin 1 gene is related to creativity in people with high intellectual achievement. Psychol. Sci. *20*, 1070–1073.

Koshibu, K., Ahrens, E.T., and Levitt, P. (2005). Postpubertal sex differentiation of forebrain structures and functions depend on transforming growth factor-α. J. Neurosci. *25*, 3870–3880.

Krug, A., Markov, V., Leube, D., Zerres, K., Eggermann, T., Nothen, M.M., Skowronek, M.H., Rietschel, M., and Kircher, T. (2008). Genetic variation in the schizophrenia-risk gene neuregulin1 correlates with personality traits in healthy individuals. Eur. Psychiatry *23*, 344–349.

Lewis, D.A., and Levitt, P. (2002). Schizophrenia as a disorder of neurodevelopment. Annu. Rev. Neurosci. *25*, 409–432.

Lewis, D.A., Hashimoto, T., and Volk, D.W. (2005). Cortical inhibitory neurons and schizophrenia. Nat. Rev. Neurosci. *6*, 312–324.

Lipska, B.K., Jaskiw, G.E., and Weinberger, D.R. (1993). Postpubertal emergence of hyperresponsiveness to stress and to amphetamine after neonatal excitotoxic hippocampal damage: a potential animal model of schizophrenia. Neuropsychopharmacology *9*, 67–75.

Lisman, J.E., Coyle, J.T., Green, R.W., Javitt, D.C., Benes, F.M., Heckers, S., and Grace, A.A. (2008). Circuit-based framework for understanding neurotransmitter and risk gene interactions in schizophrenia. Trends Neurosci. *31*, 234–242.

LoTurco, J., Manent, J.B., and Sidiqi, F. (2009). New and improved tools for in utero electroporation studies of developing cerebral cortex. Cereb. Cortex *19* (*Suppl 1*), i120–i125.

Manent, J.B., Wang, Y., Chang, Y., Paramasivam, M., and LoTurco, J.J. (2009). Dcx reexpression reduces subcortical band heterotopia and seizure threshold in an animal model of neuronal migration disorder. Nat. Med. *15*, 84–90.

Mao, Y., Ge, X., Frank, C.L., Madison, J.M., Koehler, A.N., Doud, M.K., Tassa, C., Berry, E.M., Soda, T., Singh, K.K., et al. (2009). Disrupted in schizophrenia 1 regulates neuronal progenitor proliferation via modulation of GSK3β/β-catenin signaling. Cell *136*, 1017–1031.

Marin, O., and Rubenstein, J.L. (2003). Cell migration in the forebrain. Annu. Rev. Neurosci. *26*, 441–483.

Matsuda, T., and Cepko, C.L. (2007). Controlled expression of transgenes introduced by in vivo electroporation. Proc. Natl. Acad. Sci. USA *104*, 1027–1032.

McNeil, T.F. (1995). Perinatal risk factors and schizophrenia: selective review and methodological concerns. Epidemiol. Rev. *17*, 107–112.

Miyamoto, Y., Yamada, K., Noda, Y., Mori, H., Mishina, M., and Nabeshima, T. (2002). Lower sensitivity to stress and altered monoaminergic neuronal function in mice lacking the NMDA receptor ε 4 subunit. J. Neurosci. *22*, 2335–2342.

Miyamoto, Y., Yamada, K., Nagai, T., Mori, H., Mishina, M., Furukawa, H., Noda, Y., and Nabeshima, T. (2004). Behavioural adaptations to addictive drugs in mice lacking the NMDA receptor ε1 subunit. Eur. J. Neurosci. *19*, 151–158.

Moore, H., Jentsch, J.D., Ghajarnia, M., Geyer, M.A., and Grace, A.A. (2006). A neurobehavioral systems analysis of adult rats exposed to methylazoxymethanol acetate on E17: implications for the neuropathology of schizophrenia. Biol. Psychiatry *60*, 253–264.

Navarro-Quiroga, I., Chittajallu, R., Gallo, V., and Haydar, T.F. (2007). Long-term, selective gene expression in developing and adult hippocampal pyramidal neurons using focal in utero electroporation. J. Neurosci. *27*, 5007–5011.

Niwa, M., Nitta, A., Mizoguchi, H., Ito, Y., Noda, Y., Nagai, T., and Nabeshima, T. (2007). A novel molecule "shati" is involved in methamphetamine-induced hyperlocomotion, sensitization, and conditioned place preference. J. Neurosci. *27*, 7604–7615.

Owen, M.J., Craddock, N., and O'Donovan, M.C. (2005). Schizophrenia: genes at last? Trends Genet. *21*, 518–525.

Ozawa, K., Hashimoto, K., Kishimoto, T., Shimizu, E., Ishikura, H., and Iyo, M. (2006). Immune activation during pregnancy in mice leads to dopaminergic hyperfunction and cognitive impairment in the offspring: a neurodevelopmental animal model of schizophrenia. Biol. Psychiatry *59*, 546–554.

Ozeki, Y., Tomoda, T., Kleiderlein, J., Kamiya, A., Bord, L., Fujii, K., Okawa, M., Yamada, N., Hatten, M.E., Snyder, S.H., et al. (2003). Disrupted-in-Schizophrenia-1 (DISC1): mutant truncation prevents binding to NudE-like (NUDEL) and inhibits neurite outgrowth. Proc. Natl. Acad. Sci. USA *100*, 289–294.

Rapoport, J.L., Addington, A.M., Frangou, S., and Psych, M.R. (2005). The neurodevelopmental model of schizophrenia: update 2005. Mol. Psychiatry *10*, 434–449.

Rayevsky, K.S., Gainetdinov, R.R., Grekhova, T.V., and Sotnikova, T.D. (1995). Regulation of dopamine release and metabolism in rat striatum in vivo: effects of dopamine receptor antagonists. Prog. Neuropsychopharmacol. Biol. Psychiatry *19*, 1285–1303.

Rosenberg, D.R., and Lewis, D.A. (1995). Postnatal maturation of the dopaminergic innervation of monkey prefrontal and motor cortices: a tyrosine hydroxylase immunohistochemical analysis. J. Comp. Neurol. *358*, 383–400.

Sauvageot, C.M., and Stiles, C.D. (2002). Molecular mechanisms controlling cortical gliogenesis. Curr. Opin. Neurobiol. *12*, 244–249.

Savitz, J., and Drevets, W.C. (2009). Bipolar and major depressive disorder: neuroimaging the developmental-degenerative divide. Neurosci. Biobehav. Rev. *33*, 699–771.

Selemon, L.D., and Goldman-Rakic, P.S. (1999). The reduced neuropil hypothesis: a circuit based model of schizophrenia. Biol. Psychiatry *45*, 17–25.

Sesack, S.R., Carr, D.B., Omelchenko, N., and Pinto, A. (2003). Anatomical substrates for glutamate-dopamine interactions: evidence for specificity of connections and extrasynaptic actions. Ann. N Y Acad. Sci. *1003*, 36–52.

Shu, T., Ayala, R., Nguyen, M.D., Xie, Z., Gleeson, J.G., and Tsai, L.H. (2004). Ndel1 operates in a common pathway with LIS1 and cytoplasmic dynein to regulate cortical neuronal positioning. Neuron *44*, 263–277.

Tabata, H., and Nakajima, K. (2001). Efficient in utero gene transfer system to the developing mouse brain using electroporation: visualization of neuronal migration in the developing cortex. Neuroscience *103*, 865–872.

Tenyi, T., Trixler, M., and Csabi, G. (2009). Minor physical anomalies in affective disorders. A review of the literature. J. Affect. Disord. *112*, 11–18.

Tomppo, L., Hennah, W., Miettunen, J., Jarvelin, M.R., Veijola, J., Ripatti, S., Lahermo, P., Lichtermann, D., Peltonen, L., and Ekelund, J. (2009). Association of variants in DISC1 with psychosis-related traits in a large population cohort. Arch. Gen. Psychiatry *66*, 134–141.

Tsai, J.W., Chen, Y., Kriegstein, A.R., and Vallee, R.B. (2005). LIS1 RNA interference blocks neural stem cell division, morphogenesis, and motility at multiple stages. J. Cell Biol. *170*, 935–945.

Tseng, K.Y., Lewis, B.L., Hashimoto, T., Sesack, S.R., Kloc, M., Lewis, D.A., and O'Donnell, P. (2008). A neonatal ventral hippocampal lesion causes functional deficits in adult prefrontal cortical interneurons. J. Neurosci. *28*, 12691–12699.

White, T., Anjum, A., and Schulz, S.C. (2006). The schizophrenia prodrome. Am. J. Psychiatry *163*, 376–380.

Young-Pearse, T.L., Bai, J., Chang, R., Zheng, J.B., LoTurco, J.J., and Selkoe, D.J. (2007). A critical function for β-amyloid precursor protein in neuronal migration revealed by in utero RNA interference. J. Neurosci. *27*, 14459–14469.

Yu, Z.X., Li, S.H., Evans, J., Pillarisetti, A., Li, H., and Li, X.J. (2003). Mutant huntingtin causes context-dependent neurodegeneration in mice with Huntington's disease. J. Neurosci. *23*, 2193–2202.

Neuron, Volume 65 Supplemental Information

Knockdown of DISC1 by In Utero Gene Transfer Disturbs Postnatal Dopaminergic Maturation in the Frontal Cortex and Leads to Adult Behavioral Deficits

Minae Niwa, Atsushi Kamiya, Rina Murai, Ken-ichiro Kubo, Aaron J. Gruber, Kenji Tomita, Lingling Lu, Shuta Tomisato, Hanna Jaaro-Peled, Saurav Seshadri, Hideki Hiyama, Beverly Huang, Kazuhisa Kohda, Yukihiro Noda, Patricio O'Donnell, Kazunori Nakajima, Akira Sawa, and Toshitaka Nabeshima

SUPPLEMENTARY FIGURES

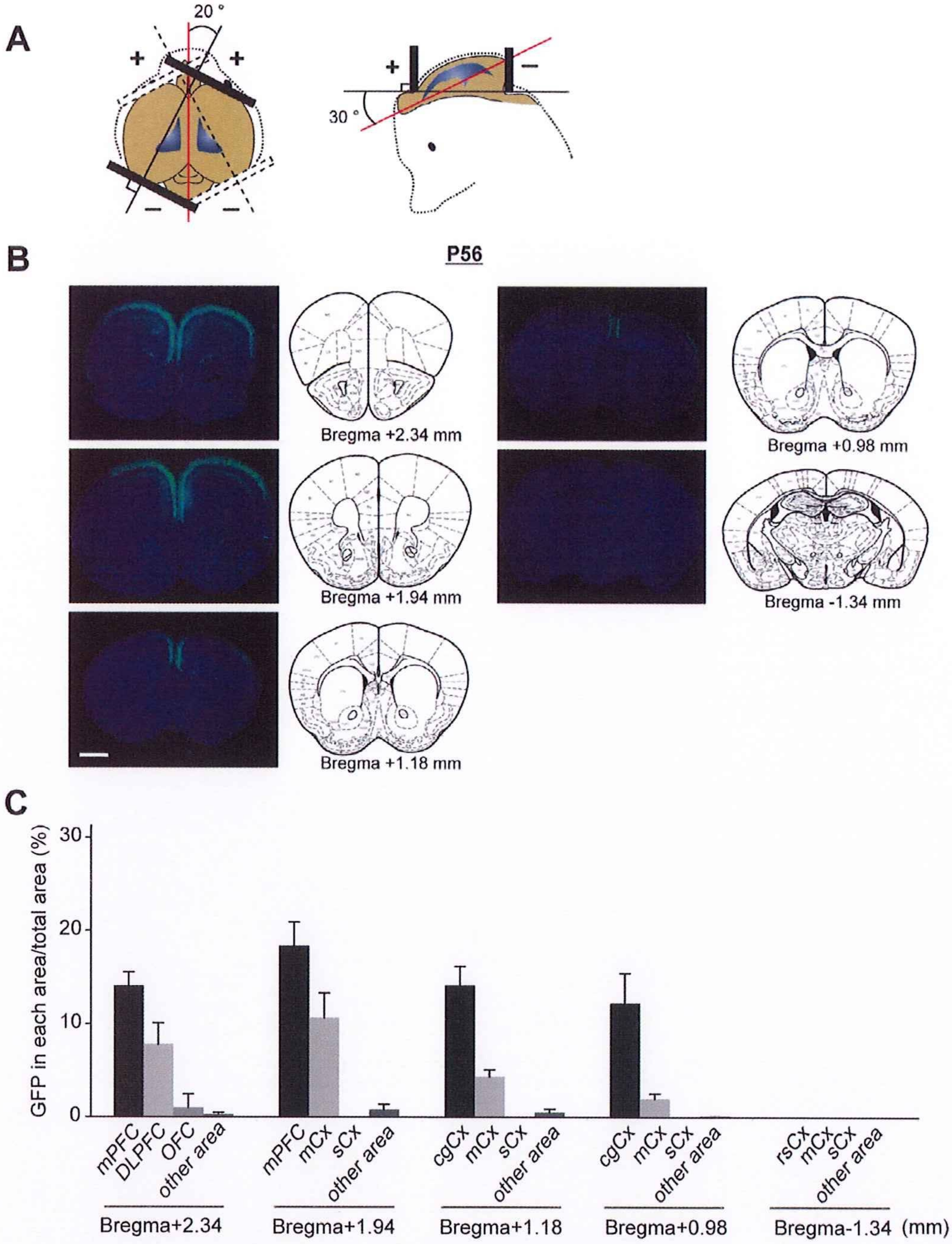

Figure S1. Application of *in utero* gene transfer for modulating gene expression mainly in prefrontal cortex (PFC)
(A) Schematic representation of bilateral *in utero* electroporation at embryonic day 14 (E14). The embryo's head in the uterus was held with a forceps-type electrode, consisting of two disc electrodes. The electrodes were oriented at a rough 20 degree outward angle from the midline and a rough 30 degree angle downward from an imaginary line from the olfactory bulbs to the caudal side of cortical hemisphere. (B) Representative rostral-caudal image series of coronal sections of brains with GFP expression at postnatal day 56 (P56) (+2.34 mm, +1.94 mm, +1.18 mm, +0.98 mm, and -1.34 mm from Bregma). Blue, nucleus. Scale bar, 1mm. (C) Distribution of GFP-positive cells in series of coronal sections of brains at P56. GFP -positive area is mainly in PFC, including medial prefrontal cortex (mPFC), dorsolateral prefrontal cortex (DLPFC), orbitofrontal cortex (OFC), and cingulate cortex (cgCx). mCx, motor cortex; sCx, sensory cortex; rsCx, retrosplenial cortex. N=6 per each coronal section. Error bars show mean + SEM.

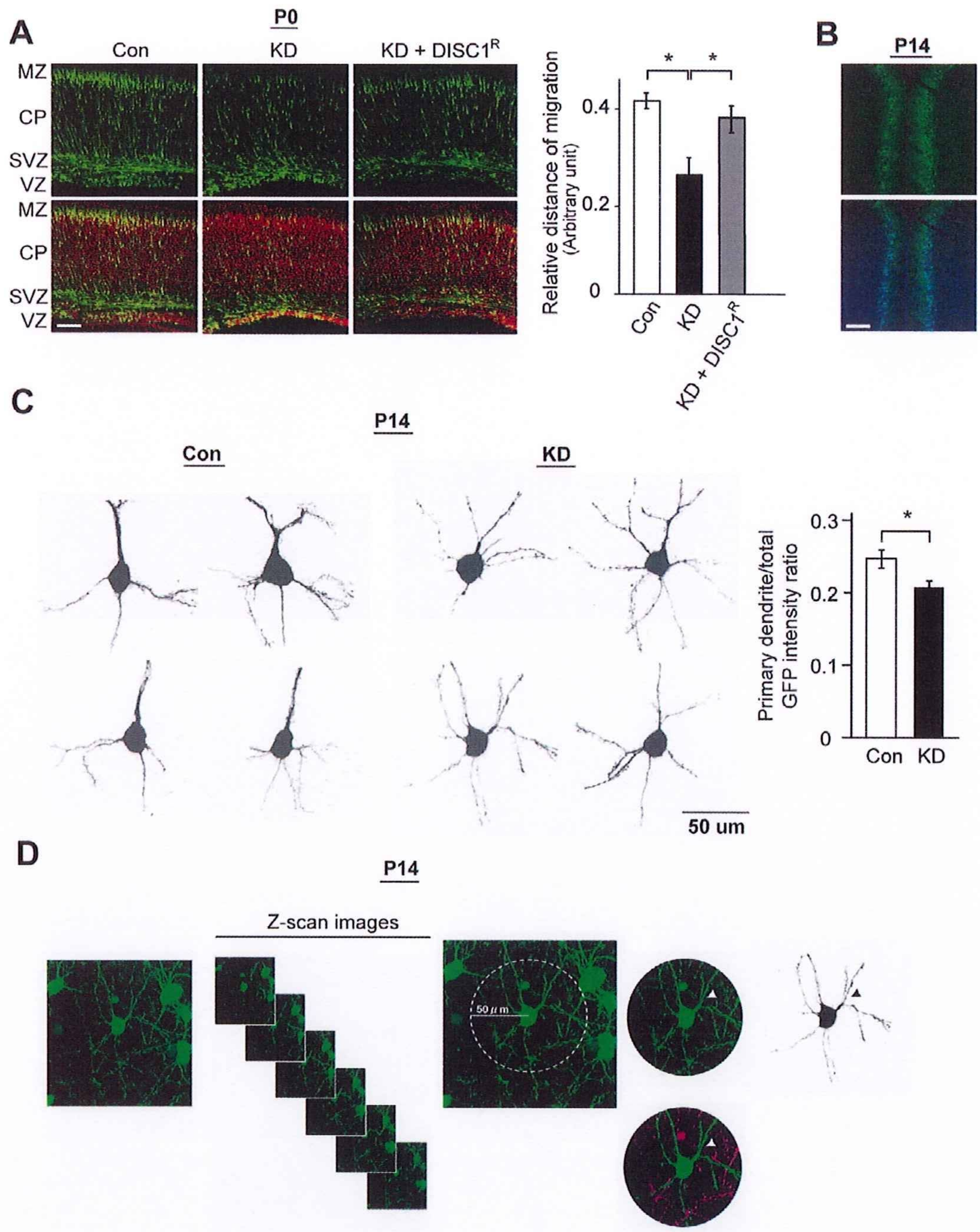
A
P0
Con
KD
KD + DISC1^R
MZ
CP
SVZ
VZ
Relative distance of migration (Arbitrary unit)
0.4
0.2
0
Con
KD
KD + DISC1^R
B
P14
C
P14
Con
KD
Primary dendrite/total GFP intensity ratio
0.3
0.2
0.1
0
Con
KD
50 um
D
P14
Z-scan images
50 μm

Figure S2. Impaired dendritic morphology of pyramidal neurons in DISC1 KD mice

(A) DISC1 shRNA-elicited impaired cortical development (here, migration defect was assayed at P0) was normalized by co-electroporation of RNAi-resistant wild-type DISC1 ($DISC1^R$) (*p<0.01). N=5 per condition. MZ, marginal zone; CP, cortical plate; SVZ, subventricular zone; VZ, ventricular zone. Con, control. Red, nucleus. Scale bar, 30 μm. Error bars show mean + SEM. (B) Representative coronal images of mPFC with GFP expression at postnatal day 14 (P14). Blue, nucleus. Scale bar, 200 μm. (C) Left, representative reconstructed images of GFP-positive neurons in mPFC at P14 in DISC1 KD and Con mice. Right, the ratio of GFP signal intensity of the primary dendrite to that of the whole cell area (processes and the cell body) is decreased in KD compared with Con mice (*p<0.01). N=10 per condition. Error bars show mean + SEM. (D) Schema of morphological analysis of dendrites. Compiled pictures of focal plane z-stacks (10 μm thick) taken at 2μm intervals were analyzed. GFP-positive dendrites originating from other adjacent GFP-positive neurons (magenta) were distinguished based on observation of uncompressed z-scan images, and were manually erased. In each GFP-positive neuron, the ratio of GFP signal intensity between the main apical shaft of dendrites (arrowheads) and the area inside a circle with 50 μm diameter centered on the cell body was measured.

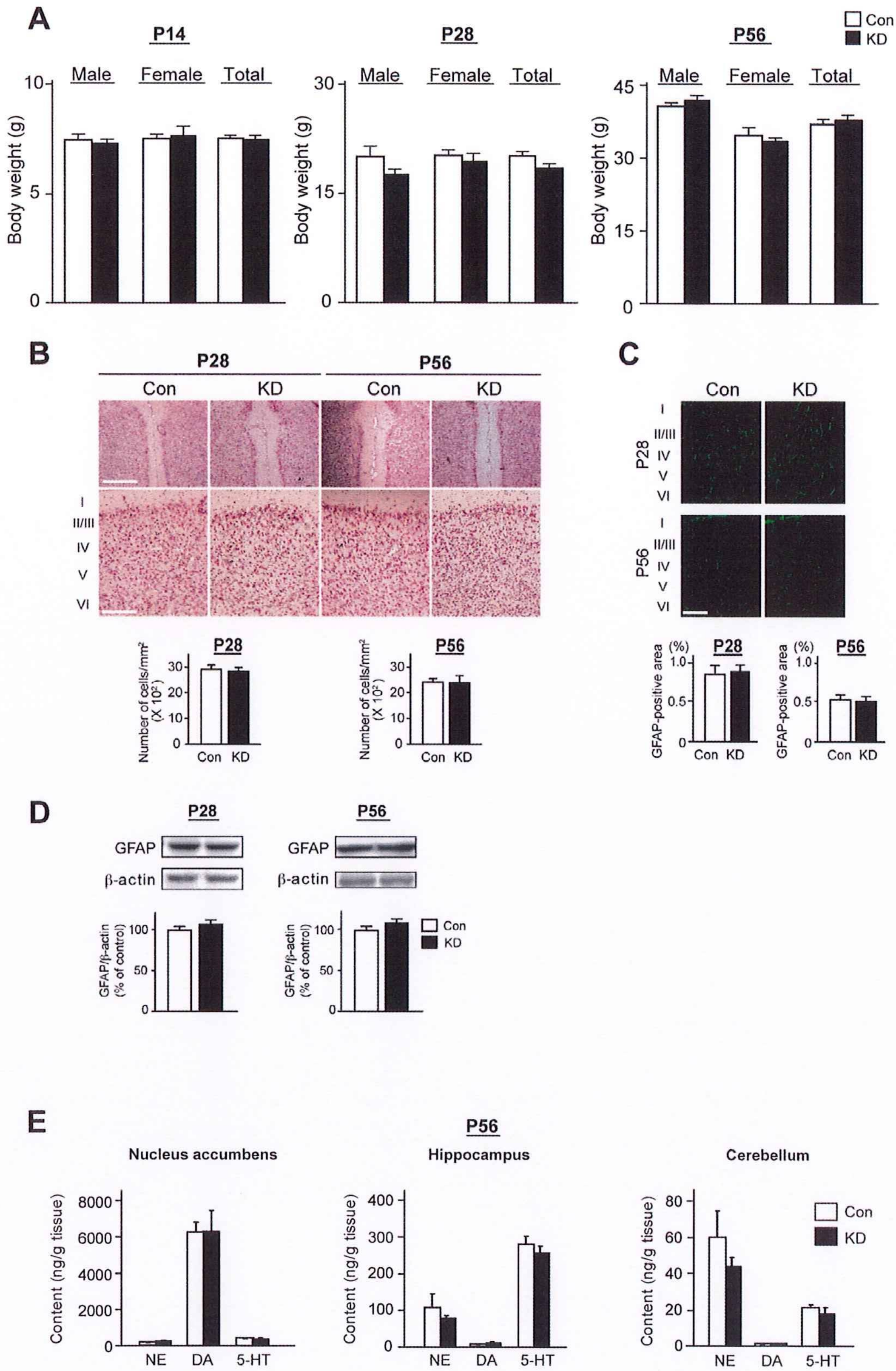

A
P14
P28
P56
Con
KD
Male
Female
Total
Body weight (g)
B
P28
P56
Con
KD
I
II/III
IV
V
VI
Number of cells/mm² (X 10²)
C
GFAP-positive area (%)
D
GFAP
β-actin
GFAP/β-actin (% of control)
E
Nucleus accumbens
Hippocampus
Cerebellum
Content (ng/g tissue)
NE
DA
5-HT

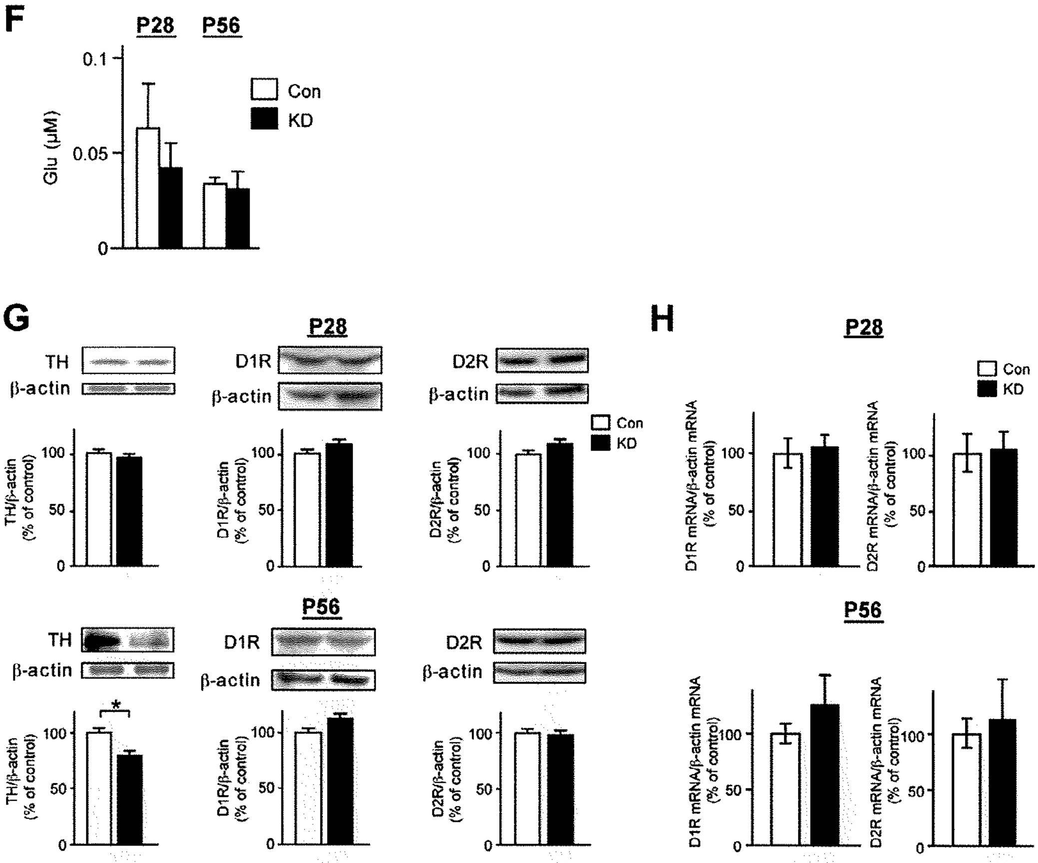

Figure S3. Evaluation of Body weight, gross anatomical and neurochemical changes in DISC1 KD mice
(A) There was no significant difference in weight between DISC1 KD mice and Con mice at P14, P28, and P56. There was no significant difference in weight between genders. N=24-60 (male) and N=31-74 (female) per condition. (B) Nissl staining in mPFC. Representative sections with cresyl violet throughout prelimbic and infralimbic cortex are shown at low magnification (upper panels) and high magnification (bottom panels). There were no robust anatomical changes in DISC1 KD mice compared with Con mice at P28 and P56. N=6 per condition. Scale bars, low magnification, 500 μm; high magnification, 200 μm. (C) Immunostaining of glial fibrial acidic protein (GFAP) in mPFC. There was no difference in the expression levels of GFAP in DISC1 KD (right panels) and Con mice (left panels) at P28 and P56. N=6 per condition. Scale bars: 200 μm. (D) No differences in the expression levels of GFAP in frontal cortex (FC) between DISC1 KD and Con mice at P28 and P56 were detected by Western blotting. N=5 per condition. (E) Monoamine content in nucleus accumbens, hippocampus, and cerebellum in DISC1 KD mice at P56. Norepinephrine (NE), dopamine (DA), and 5-hydroxytryptamine (5-HT) were analyzed using high-performance liquid chromatography (HPLC). There was no difference in the contents of NE, DA, and 5-HT in these regions between DISC1 KD and Con mice. N=4 per condition. (F) Basal levels of extracellular glutamate (Glu) in mPFC were analyzed by *in vivo* microdialysis. There was no difference in basal level of Glu in mPFC between DISC1 KD and Con mice at P28 and P56. N=4 per condition. (G) Protein expression levels of tyrosine hydroxylase (TH), dopamine D1 receptor (D1R), and D2 receptor (D2R) in FC. The expression level of TH was decreased in FC of DISC1 KD mice at P56, but not P28, in comparison with Con mice (*$p<0.05$). There was no difference in the expression levels of D1R and D2R between DISC1 KD and Con mice at P28 and P56. N=5 per condition. (H) The mRNA expression levels of D1R and D2R in FC. There were no differences in the mRNA expression levels of D1R and D2R between DISC1 KD and Con mice at P28 and P56. N=8 per condition. Error bars show mean + SEM.

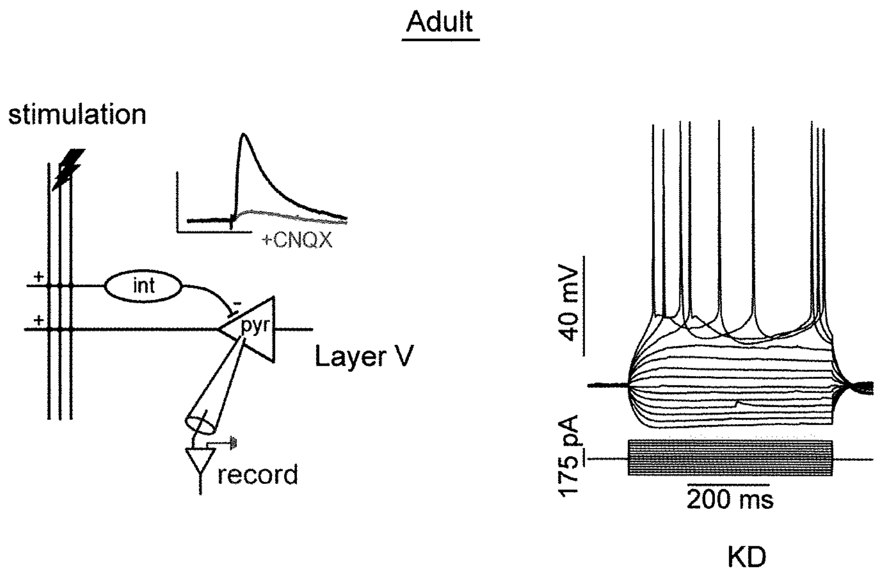

Figure S4. Electrophysiological responses of pyramidal neurons in mPFC in adult DISC1 KD mice
Left, illustration of the experimental configuration showing relative location of stimulation in superficial layers of mPFC with respect to intracellular recording from a deep layer pyramidal neuron (left panel). Stimulation can activate pyramidal neurons (pyr) as well as GABAergic interneurons (int), both of which can contribute to evoked responses. Application of the AMPA/kainate antagonist CNQX blocked evoked responses (inset), confirming them to be synaptically mediated. Scale bars, 5 mV and 100 msec. Right, membrane potential responses of a representative deep layer mPFC pyramidal neuron to current pulses in an acute slice preparation from an adult DISC1 KD mouse are shown as overlapping traces.

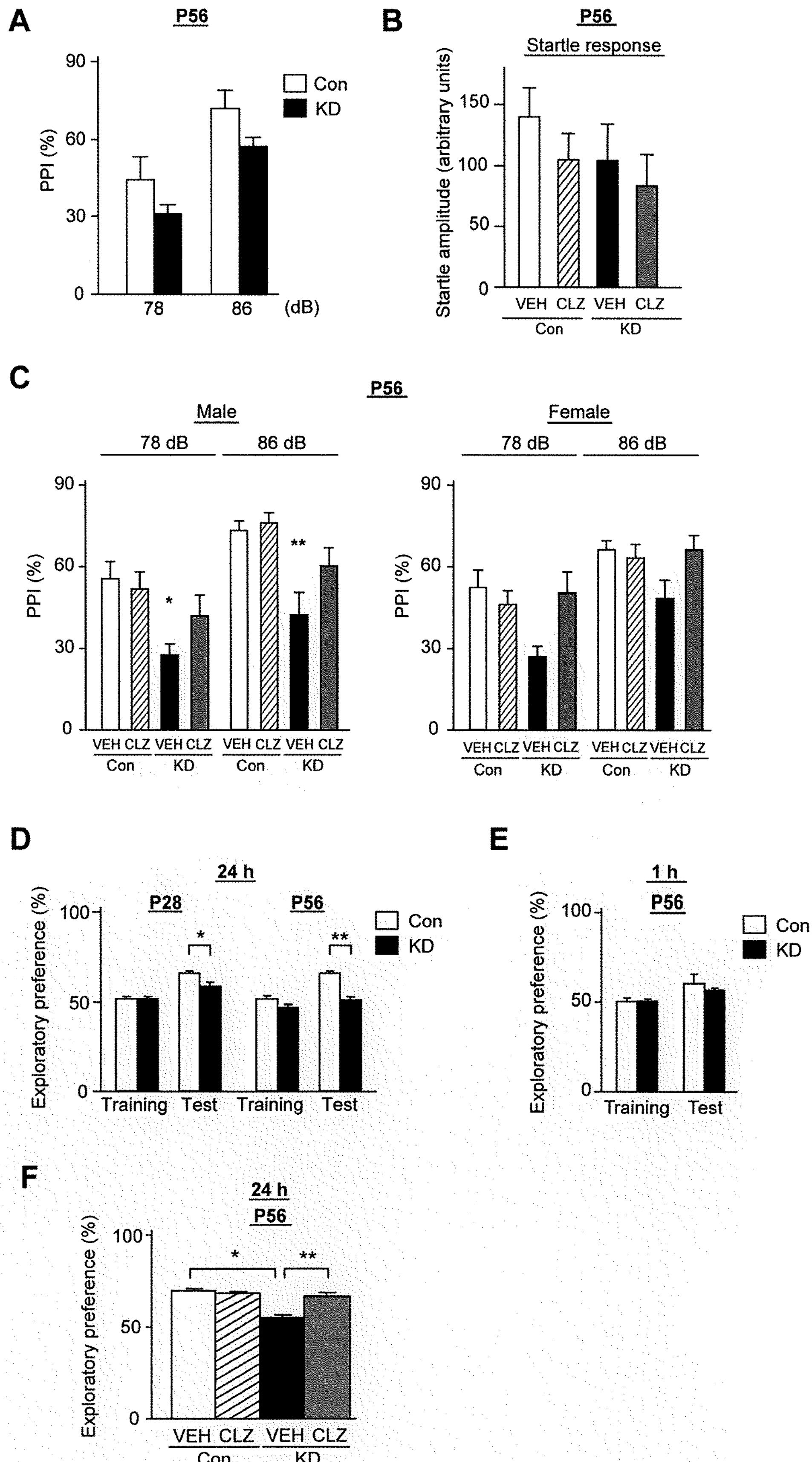

A
P56
PPI (%)
90
60
30
0
Con
KD
78
86
(dB)
B
P56
Startle response
Startle amplitude (arbitrary units)
150
100
50
0
VEH CLZ VEH CLZ
Con
KD
C
P56
Male
Female
78 dB
86 dB
PPI (%)
90
60
30
0
*
**
VEH CLZ VEH CLZ VEH CLZ VEH CLZ
Con KD Con KD
D
24 h
P28
P56
Exploratory preference (%)
100
50
0
*
**
Con
KD
Training Test Training Test
E
1 h
P56
Exploratory preference (%)
100
50
0
Con
KD
Training Test
F
24 h
P56
Exploratory preference (%)
100
50
0
*
**
VEH CLZ VEH CLZ
Con
KD